ELSEVIER

Solid State Ionics 152–153 (2002) 311–318

SOLID STATE IONICS

www.elsevier.com/locate/ssi

Hydrothermal synthesis of high crystalline orthorhombic $LiMnO_2$ as a cathode material for Li-ion batteries

Shinichi Komaba [a,*], Seung-Taek Myung [a], Naoaki Kumagai [a], Toru Kanouchi [a], Kenichi Oikawa [b], Takashi Kamiyama [b]

[a] *Department of Chemical Engineering, Faculty of Engineering, Iwate University, 4-3-5 Ueda, Morioka, Iwate 020-8551, Japan*
[b] *Neutron Science Laboratory, Institute of Materials Structure Science, High Energy Accelerator Research Organization, 1-1 Oho, Tsukuba, Ibaraki 305-0801, Japan*

Accepted 15 March 2002

Abstract

A low-temperature, hydrothermal process for the synthesis of high-quality intercalation oxide $LiMnO_2$ has been developed. Mn_3O_4 as a hydrothermal precursor was prepared by oxidation of $Mn(OH)_2$ by bubbling O_2 at 80 °C. The fine single crystalline particle oxide, Mn_3O_4, was hydrothermally treated with various LiOH concentrations at 170 °C. The mechanism of phase evolution has been studied by using X-ray diffraction (XRD) and transmission electron microscopy (TEM). Rietveld analysis revealed that a well-ordered orthorhombic $LiMnO_2$ having a zigzag layer structure (*Pmnm*) was readily formed by hydrothermal reaction. The product is electrochemically active and shows relatively high capacity upon cycling.

Keywords: Hydrothermal process; Mn_3O_4; Lithium intercalation; Orthorhombic $LiMnO_2$; Electrochemistry

1. Introduction

With help of remarkable development of technologies, demands for portable devices are tremendously increasing. Here, what we must think is Li-ion secondary batteries as power sources are being adopted in these cordless portable devices. How to satisfy the demand? The answer is to supply good power sources that can offer long cycle life, light weight, cheapness and environmental kindness. So, there are several kinds of cathode materials for Li-ion secondary batteries to fulfill the conditions. Among them, spinel-type $LiMn_2O_4$ is the best candidate. However, the material has a poor cyclability due mainly to the collective Jahn-Teller distortion when it cycles below 3 V.

A zigzag layered orthorhombic $LiMnO_2$, isomorphic β-$NaMnO_2$, has a theoretical capacity twice that of $LiMn_2O_4$. The same as other materials, orthorhombic $LiMnO_2$ (hereafter referred to as *o*-$LiMnO_2$) had been studied from conventional solid-state reactions (700–1050 °C) [1,2]. Using this method, however, the powder preparation route is also quite complicated, for example, several times calcination and subsequent physical grindings. Moreover, its electrochemical properties are greatly dependent on its crystalline particle size [3]. So, low-temperature soft-chemistry routes were employed to enhance its electrochemical properties. Much enhanced battery

Corresponding author. Tel.: +81-19-621-6329; fax: +81-19-621-6328.
E-mail address: komaba@iwate-u.ac.jp (S. Komaba).

0167-2738/02/$ - see front matter © 2002 Elsevier Science B.V. All rights reserved.
PII: S0167-2738(02)00320-X

performances were surely obtained [4,5]. However, there remained one problem unsolved, that is, high-capacity retention upon cycling.

Until now, there are a few reports concerning high-capacity maintainable orthorhombic $LiMnO_2$ synthesized by calcination of freeze-dried precursor at 950 °C [6]. In this case, the powder preparation is too difficult, because it needs well-controlled oxygen partial pressure (about $P_{O_2}=10^{-6}$ atm).

This point prompted us to consider a mild preparation route to synthesize the oxide powder, namely, hydrothermal treatment, which is a kind of promising technique for synthesis of lithium transition metal oxide cathodes. Here, for the first time, *o*-$LiMnO_2$ was synthesized from Mn_3O_4 by hydrothermal route at 170 °C.

2. Experimental

To prepare Mn_3O_4 as a hydrothermal reaction precursor, manganese hydroxide was oxidized through a mild oxidation route [7]. Details of powder preparation sequence are described in our previous report [8]. Manganese acetate tetrahydrate ($Mn(CH_3COO)_2{\cdot}4H_2O$, R.G. of Kanto Chemicals) was dissolved in distilled water. Then, the manganese solution (100 ml) was mixed with 10 M potassium hydroxide aqueous solution (50 ml), and the aqueous solution mixture was stirred at 80 °C for 1 day with bubbling O_2 gas to promote manganese oxidation, and finally dark brown Mn_3O_4 powders precipitated on the bottom of reactor. The precipitates were continuously washed with deionized water until pH reaches neutral and dried at 80 °C in air. The prepared Mn_3O_4 powders (0.2 g) were hydrothermally treated with various concentrations of $LiOH{\cdot}H_2O$ (R.G. of Wako) aqueous solution at 170 °C for 4 days in autoclaves. A Teflon beaker was used to avoid any reaction with the vessel. After hydrothermal reaction, the precipitates were washed with deionized water, and the products were dried to remove water at 120 °C in air.

To understand structure of the prepared materials, X-ray powder diffraction (XRD) was carried out using a Cu Kα radiation of Rigaku Rint 2200 diffractometer. The collected intensity data were analyzed by the Rietveld refinement program, RIETAN 2000 [9]. Transmission electron microscopy (TEM; Hitachi, H-800) observation was carried out to check the products. Pieces of the fresh powders were ultrasonically de-agglomerated and dispersed on an amorphous carbon grid supported by a Cu frame for TEM observation. The accelerated voltage of electron beam used was 200 kV. Atomic absorption spectroscopy (AAS, Analyst 300, Perkin Elmer) was employed to analyze chemical composition of the *o*-$LiMnO_2$.

For electrochemical testing in Li cell, working electrodes were fabricated by mixing the prepared *o*-$LiMnO_2$ powder, graphite, acetylene black and polyvinylidene fluoride in NMP, as described in our previous report [8]. The slurry was pasted on nickel ex-met (1 cm^2), and the electrode was dried to evaporate NMP component at 80 °C for 1 day, and then dried again at 120 °C for 4 days in vacuum state. The cell consisted of the oxide cathode as a working electrode and lithium ribbon as a counter electrode was assembled in Ar-filled glove box. The cells filled with 1 M $LiClO_4$ in EC-DEC (1:1, Tomiyama) as electrolyte were charged and discharged between 2.0 and 4.3 V_{Li/Li^+} at a current density 0.1 mA cm^{-2} (45 mA g^{-1}) at 25 °C.

3. Results and discussion

3.1. Oxidation of manganese hydroxide precipitated by potassium hydroxide

A precipitate of $Mn(OH)_2$ was formed immediately by mixing 1 M manganese acetate solution and 10 M KOH solution. The oxygen bubbling was employed to oxidize $Mn(OH)_2$ much faster at 80 °C in KOH solution. According to the previous report [7], a reaction at elevated temperature with an excess of hydroxide ions and oxygen gas, where $Mn(OH)_2$ precipitated, is fairly effective to get purer forms of manganese oxides such as MnO_2, Mn_2O_3 and Mn_3O_4. After washing the precipitates with deionized water until the pH reaches to neutral, Mn_3O_4 appears as the major phase with no other Mn-containing minor phases being detectable. Fig. 1a shows the XRD pattern of Mn_3O_4 after autoxidation of $Mn(OH)_2$ at 80 °C. Here, we think possible reaction route as follows:

$$6Mn(OH)_2 + O_2 \rightarrow 2Mn_3O_4 + 6H_2O \quad (1)$$

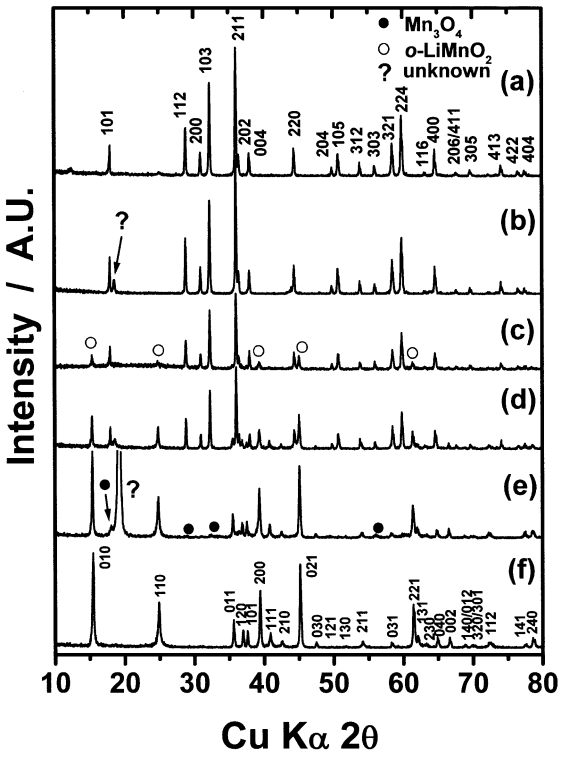

Fig. 1. XRD patterns indicating phase evolution from Mn_3O_4 to *o*-$LiMnO_2$ by hydrothermal reaction between Mn_3O_4 and various concentrations of LiOH aqueous solution at 170 °C for 4 days; (a) as-prepared Mn_3O_4, (b) 0.1, (c) 1, (d) 2, (e) 3 and (f) 3.5 M.

Miller indices (*hkl*) are given for the spinel-type tetragonal phase with a space group of $I4_1/amd$ in Fig. 1 [10]. The calculated lattice parameters from the XRD pattern are a= 5.7676 Å, and c= 9.4889 Å, which are well coincident with the JCPDS card [10,11].

3.2. Hydrothermal treatment of the Mn_3O_4

To figure out how *o*-$LiMnO_2$ phase can be formed from Mn_3O_4 by reacting with LiOH aqueous solution, powder XRDs were taken as a function of LiOH aqueous concentration as a solvent (Fig. 1). TEM observation was accompanied to observe the phase evolution steps directly, as shown in Fig. 2. Selected-area diffraction (SAD) pattern showed that the Mn_3O_4 prepared by autoxidation route illustrates a single crystallite particle with cubic shape. Its edges and corners are well developed with sharpness (Fig. 2a). When the concentration was 0.1 M, it seems that no reaction occurred. Its corresponding TEM photo also depicts that there is no significant change in particle shape and size (Fig. 2b). As can be seen in Fig. 1c, the *o*-$LiMnO_2$ phase marked with open circle begins to appear as a minor phase. TEM picture also showed somehow different particle shapes in Fig. 2c. Some of particles lost their sharpness in their corners, compared with Fig. 2a and b. It is able to think that some parts of the precursor allow lithium ion to be incorporated into the structure during hydrothermal reaction. As the concentration of LiOH increased, the *o*-$LiMnO_2$ phase appeared more and more. When the concentration was 3 M, the diffraction pattern shows *o*-$LiMnO_2$ phase as a major phase and Mn_3O_4 as a minor phase. Corners of particles showed rounded shape (see Fig. 2d and e). When the concentration reached 3.5 M, the XRD pattern revealed that the most of Mn_3O_4 has been transformed to the layered *o*-$LiMnO_2$ phase. As confirmed by TEM, corners of particles changed to more rounded shape and their particle size was smaller than precursor Mn_3O_4, as seen in Fig. 2f. SAD pattern of *o*-$LiMnO_2$ also suggests that each particle of the prepared oxide by hydrothermal treatment is a single crystal.

There is a possible way to explain how the *o*-$LiMnO_2$ phase could be formed from the aqueous solution; partial dissolution of Mn^{2+} from the Mn_3O_4 precursor which consists of spinel $Mn^{2+}[Mn^{3+}]_2O_4$ (average valence of Mn: 2.67) into the strong basic aqueous LiOH solution with combination of direct incorporation of lithium ions into the tetragonal Mn_3O_4 structure as the following chemical equation:

$$Mn^{2+}[Mn^{3+}]_2O_4 + 2Li^+ \rightarrow 2LiMnO_2 + Mn^{2+} \quad (2)$$

Only when the concentration of lithium salt in aqueous solution is 3.5 M, the pure *o*-$LiMnO_2$ phase could be formed, as confirmed by XRD in Fig. 1. That is, the 3.5 M of LiOH aqueous concentration used to the hydrothermal reaction may be enough to dissolve all of Mn^{2+} in $Mn^{2+}[Mn^{3+}]_2O_4$ during hydrothermal reaction.

To determine the dissolved manganese ingredient after hydrothermal reaction at 170 °C, the hydrothermally reacted aqueous solution was examined by AAS. According to the AAS results, manganese component was included in the reacted solution as shown

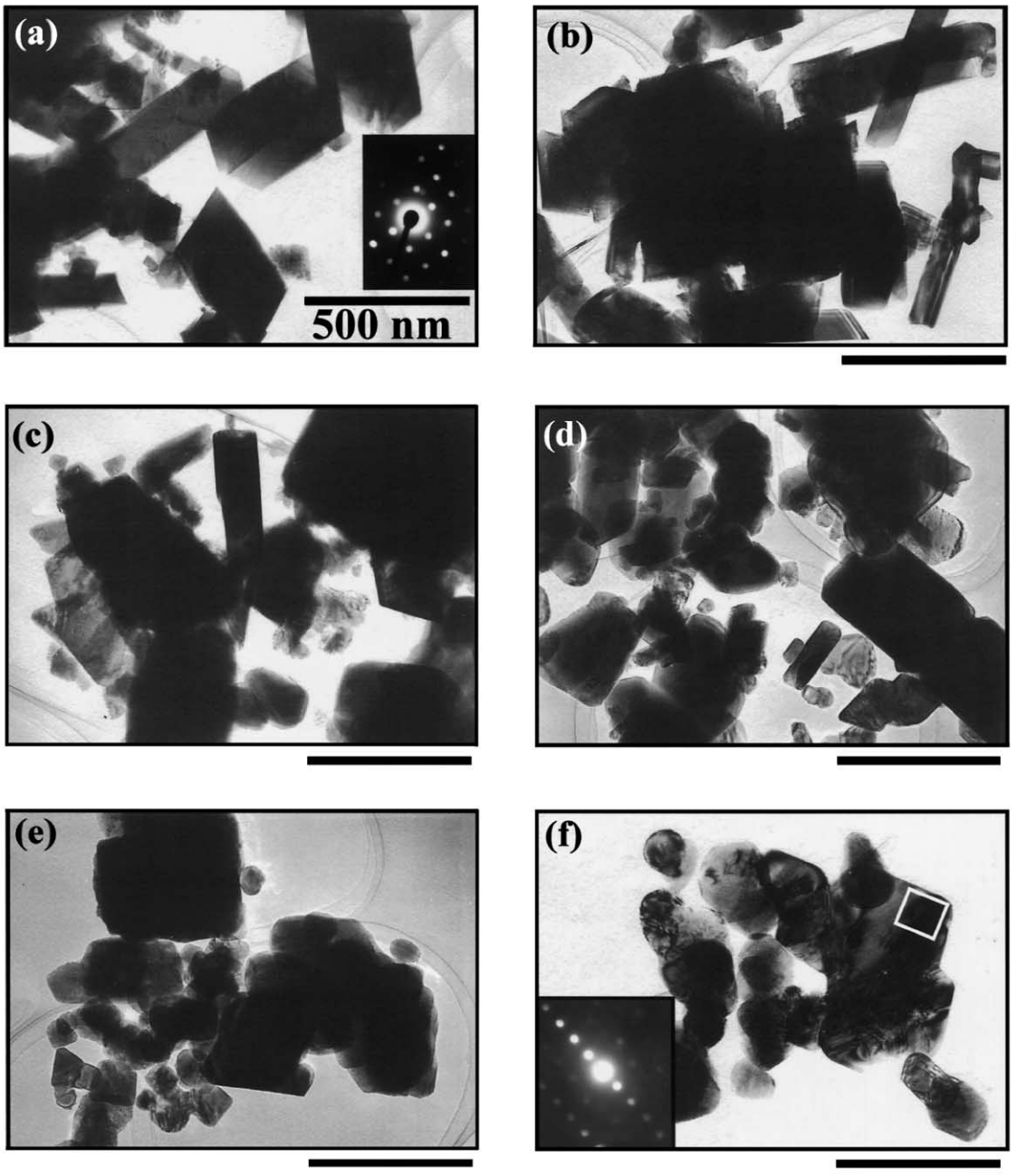

Fig. 2. TEM bright-field images of morphology evolution from Mn_3O_4 to *o*-$LiMnO_2$ by hydrothermal reaction between Mn_3O_4 and various concentrations of LiOH aqueous solution at 170 °C; (a) as-prepared Mn_3O_4, (b) 0.1, (c) 1, (d) 2, (e) 3 and (f) 3.5 M.

in Fig. 3. The dissolved Mn^{2+} in LiOH aqueous solution increased monotonously, meaning progressive phase formation of *o*-$LiMnO_2$ as mentioned in Figs. 1 and 2. It is most likely that the Mn^{2+} in $Mn^{2+}[Mn^{3+}]_2O_4$ was mostly dissolved in 3.5 M of LiOH aqueous solution, because the value 31% in

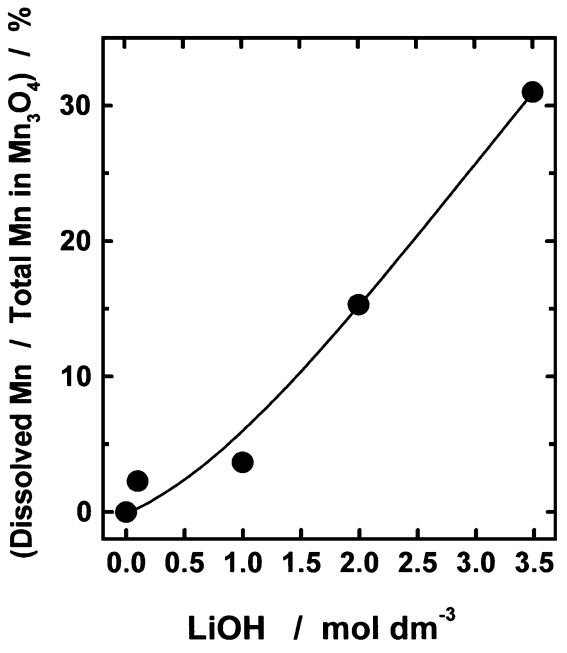

Fig. 3. Variation in dissolved Mn ratio in LiOH aqueous solution after hydrothermal reaction. The used solution for AAS was 10 ml.

(dissolved Mn)/(total Mn in the Mn_3O_4) coincides well with the theoretical value of 33% of Mn^{2+} in $Mn^{2+}[Mn^{3+}]_2O_4$. So, we believe that the most appropriate concentration of lithium aqueous solution to prepare *o*-$LiMnO_2$ is 3.5 M. Thus, the layered orthorhombic phase could be readily formed by the selective dissolution of Mn^{2+} from the spinel-type precursor $Mn^{2+}[Mn^{3+}]_2O_4$ by the hydrothermal treatment without any oxidant at low temperature as low as 170 °C.

Table 1
Structural parameters obtained from Rietveld refinement of orthorhombic $LiMnO_2$ synthesized by hydrothermal treatment at 170 °C

Formula	$Li_{1.00}Mn_{1.00}O_2$			
Crystal system	Orthorhombic			
Space group	*Pmnm*			
	a/Å	*b*/Å	*c*/Å	*V*/Å^3
	4.5795 (7)	5.7550 (8)	2.8106 (4)	74.073 (18)
Ref. 1	4.5756 (4)	5.7510 (4)	2.8062 (2)	73.8448
Atom (site)	*x*	y	z	B/Å^2
Li (2a)	1/4	0.111 (3)	1/4	0.70
Mn (2a)	1/4	0.6324 (4)	1/4	0.57 (11)
O_1 (2b)	3/4	0.1406 (14)	1/4	0.34 (12)
O_2 (2b)	3/4	0.5993 (11)	1/4	$=B(O_1)$
R_{wp}/%	10.42			
R_p/%	7.54			
S/%	1.436			

The Rietveld refinement was performed to assess the crystal structure of the prepared *o*-$LiMnO_2$ oxide. The space group of *Pmnm* was chosen as the best structural model. The resulting Rietveld refinement pattern and crystallographic parameters are given in

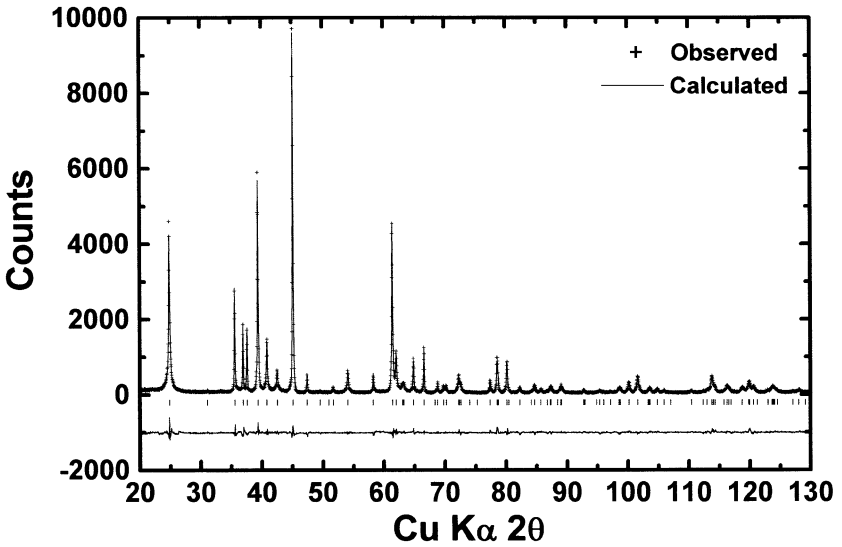

Fig. 4. Rietveld refinement of *o*-$LiMnO_2$ prepared by hydrothermal reaction between Mn_3O_4 and 3.5 M of LiOH aqueous solution at 170 °C.

Fig. 4 and Table 1, respectively. These values determined in this study are consistent with those reported in the literature [1,12]. Croguennec et al. [12,13] have pointed out that the stacking fault causes the (110) peak broadening around 25° in 2θ in XRD pattern. This asymmetry could be ascribed to the strong widening of the (110), (111) and (210) planes with particular [12]. The broadening of the peaks indicates a degree of disorder in the *o*-$LiMnO_2$ structure. As confirmed by the Rietveld analysis, *o*-$LiMnO_2$ has a well-ordered orthorhombic crystallinity. Therefore, it can be thought that this new hydrothermal condition is a very effective approach to synthesize high-quality *o*-$LiMnO_2$. Neutron diffraction studies are in progress to understand the crystal structure in more detail.

3.3. Electrochemical properties of *o*-$LiMnO_2$

Fig. 5a and b shows the charge–discharge curves and cyclability of *o*-$LiMnO_2$ electrodes at a current

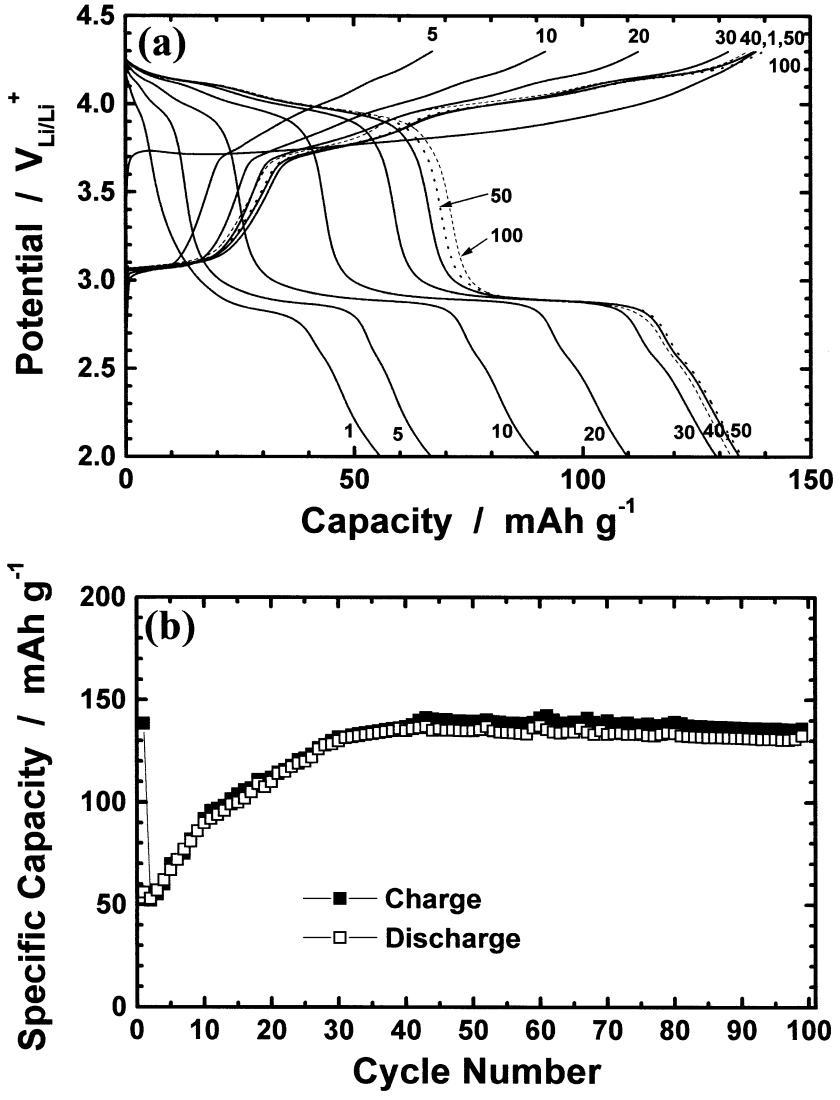

Fig. 5. (a) Charge and discharge profiles of *o*-$LiMnO_2$ and (b) its corresponding cyclability.

density of 0.1 mA cm^{-2} at 25 °C, respectively. A simple potential plateau at 3.7 V appeared in the initial charge curve. A very large capacity loss of about 95 mA h g^{-1} was observed during the first cycling, which has been previously reported by several research groups [6,14]. The polarization between charge and discharge voltages was quite large about 0.13 V. With further cycling, voltage plateaus develop more clearly at around 4 and 2.9 V, as shown in Fig. 5a, which are indications of Li intercalation on different sites, tetrahedral site over 4 V and octahedral site over 3 V into the cycle-induced spinel $LiMn_2O_4$ [15]. As shown in Fig. 5a, the spinel phase began to develop during the initial several cycles. The appearance of the 4-V plateaus contributes to increase in capacities. In more detail, the 4-V discharge plateau is gradually divided into two subplateaus, meaning that reordering of Li in the structure toward the cycle-induced spinel is in progress, as cycling goes by. The behavior is remarkably different from conventional spinel $LiMn_2O_4$ whose capacity decreases drastically within a few cyclings below the 3-V region. Furthermore, the length of the 4-V plateau is getting longer, while that of the 3-V plateau is simultaneously getting shorter with further cycling.

It seems that the present material can be cycled both over 4- and 3-V ranges without any significant capacity fading upon cycling, as can be seen in Fig. 5b. The appearance of the 4-V plateaus contributes to increase in capacities. In this way, the obtained capacities increase progressively with further cycling and stabilize after 40 cycles while showing a discharge capacity of about 140 mA h g^{-1}, proving the close properties as the *o*-$LiMnO_2$ synthesized at high temperature from freeze-dried precursor [6]. This means that the electrochemically formed spinel-like phase originated from *o*-$LiMnO_2$ is more tolerant to cycling than conventional $LiMn_2O_4$. We are subsequently developing the Co doping effect in the Mn sites by the hydrothermal method [16] and the emulsion drying synthesis of *o*-$LiMnO_2$ [17] to enhance the battery performances that will be reported in the near future.

4. Conclusion

A low-temperature hydrothermal approach using fine Mn_3O_4 and aqueous LiOH solution was shown to yield orthorhombic $LiMnO_2$ with well-ordered β-$NaMnO_2$ structure at a temperature as low as 170 °C. With increasing LiOH concentration, the most of Mn_3O_4 has been transformed to the layered *o*-$LiMnO_2$ phase, accompanied with dissolution of Mn^{2+} in LiOH aqueous solution during hydrothermal treatment, showing changes in shapes of particles from sharp to rounded corners. SAD pattern of the *o*-$LiMnO_2$ also says that each particle of the prepared oxide by hydrothermal treatment is a single crystalline particle oxide. The cyclability at a long term was excellent with help of appearance of cycle-induced spinel phase, leading to increase in capacity in the 4-V region. We believe that orthorhombic $LiMnO_2$ prepared by a new hydrothermal condition is an excellent candidate for the cathode material of coming generation with high capacity to be applied for Li-ion secondary battery.

Acknowledgements

The authors would like to thank Ms. Nobuko Kumagai, Iwate University, for her helpful assistance in the experimental work. This study was supported by Industrial Technology Research Grant Program in '00 from the New Energy and Industrial Technology Development Organization (NEDO) of Japan and Yazaki Memorial Foundation for Science and Technology.

References

[1] V.R. Hoppe, G. Brachtel, M. Jansen, Z. Anorg. Allg. Chem. 417 (1975) 1.
[2] B. Ammundsen, J. Desilvestro, T. Groutso, D. Hassell, J.B. Metson, E. Regan, R. Steiner, P.J. Pickering, J. Electrochem. Soc. 147 (2000) 4078.
[3] L. Croguennec, P. Deniard, R. Brec, J. Electrochem. Soc. 144 (1997) 3323.
[4] G. Pistoia, A. Antonini, D. Zane, Solid State Ionics 78 (1995) 115.
[5] J.N. Reimers, E.W. Fuller, E. Rossen, J.R. Dahn, J. Electrochem. Soc. 140 (1993) 3396.
[6] Y.-I. Jang, B. Huang, H. Wang, D.R. Sadoway, Y.-M. Chiang, J. Electrochem. Soc. 146 (1999) 3217.
[7] A.R. Nichols, J.H. Walton, J. Am. Chem. Soc. 64 (1942) 1866.
[8] S.-T. Myung, S. Komaba, N. Kumagai, Chem. Lett. (2001) 80–81.
[9] F. Izumi, T. Ikeda, Mater. Sci. Forum 198 (2000) 321–324.

[10] Joint Committee on Powder Diffraction Standards, File no. 24-0734.
[11] J.L. Martin de Vidales, E. Vila, R.M. Rojas, O. Garcia-Martinez, Chem. Mater. 7 (1995) 1716.
[12] L. Croguennec, P. Deniard, R. Brec, A. Lecerf, J. Mater. Chem. 7 (1995) 1919.
[13] L. Croguennec, P. Deniard, R. Brec, A. Lecerf, J. Mater. Chem. 7 (1997) 511.
[14] Z.X. Shu, I.J. Davidson, R.S. McMillan, J.J. Murray, J. Power Sources 68 (1997) 618.
[15] T. Ohzuku, M. Kitagawa, T. Hirai, J. Electrochem. Soc. 137 (1990) 769.
[16] S.-T. Myung, S. Komaba, N. Kumagai, K. Kurihara, Chem. Lett. (2001) 1114.
[17] S.-T. Myung, S. Komaba, N. Kumagai, Chem. Lett. (2001) 574.